Chapter 2. Basic Atomic Physics

Academic and Research Staff

Professor Daniel Kleppner, Professor David E. Pritchard, Professor Wolfgang Ketterle, Dr. Al-Amin Dhirani, Dr. Hans-Joachim Miesner, Dr. James V. Porto, Dr. Chandra S. Raman, Dr. Jörn Stenger, Dr. Christopher G. Townsend

Visiting Scientists and Research Affiliates

Dr. Theodore W. Ducas,[1] Roberto Onofrio

Graduate Students

Michael R. Andrews, Michael P. Bradley, Ananth P. Chikkatur, Joel C. DeVries, Dallin S. Durfee, Troy D. Hammond, Jeffrey R. Holley, Shin Inouye, David A. Kokorowski, Christopher E. Kuklewicz, Roland N. Nguyen, Simon Rainville, Tony Roberts, Richard A. Rubenstein, Edward T. Smith, Neal W. Spellmeyer, Dan M. Stamper-Kurn, James R. Thompson, Johnny M. Vogels, Huan Yao

Technical and Support Staff

Carol A. Costa

2.1 Determination of the Rydberg Frequency

Sponsor

National Science Foundation
Grant PHY 96-024740

Project Staff

Joel C. DeVries, Dr. Theodore W. Ducas, Jeffrey R. Holley, Professor Daniel Kleppner

The Rydberg constant, R_∞, relates the wavelengths of the spectrum of atomic hydrogen to practical laboratory units. As such, R_∞ is the natural unit for measurements of atomic energies and appears as an auxiliary constant in many spectroscopic measurements. The Rydberg *frequency*, cR_∞, similarly relates the atomic unit of frequency to laboratory units. Although the speed of light c is an exactly defined quantity, the relation between the Rydberg constant and the Rydberg frequency is not merely formal. Wavelength metrology appears to have reached its limit of precision, somewhat less than 1 part in 10^{11}. However, the precision with which a frequency can be measured is limited in principle only by the precision of atomic clocks, which currently exceeds 1 part in 10^{14} and is expected to grow even larger. Recent advances in optical frequency techniques have made possible measurements of cR_∞ at better than 1 part in 10^{11}.[2]

To make full use of the precision of lasers and modern laser spectroscopy and for applications in communications, control, and metrology, general techniques for measuring the frequency of light need to be developed. As part of this effort, we propose to help establish an atomic optical frequency standard by measuring the Rydberg frequency directly.

Our approach involves measuring the frequency of transitions in atomic hydrogen in a regime where the frequencies can be compared directly to an atomic clock. The experiment explores transitions between highly excited "Rydberg" states of atomic hydrogen, in the neighborhood of n=27-30. The transitions between neighboring states occur at approximately 300 GHz. This signal is generated coherently from a frequency standard based on an atomic clock. The optical measurements, in contrast, rely on intermediate standards which have been previously calibrated.

1 Professor, Wellesley College, Wellesley, Massachusetts.

2 B. de Beauvoir et al., "Absolute Frequency Measurement of the 2S–8S/D Transitions in Hydrogen and Deuterium: New Determination of the Rydberg Constant," *Phys. Rev. Lett.* 78(3): 440-43 (1997); Th. Udem et al., "Phase-Coherent Measurement of the Hydrogen 1S–2S Transition Frequency with an Optical Frequency Interval Divider Chain," *Phys. Rev. Lett.* 79(14): 2646-49 (1997).

The goals of our experiment are three-fold. First is the reevaluation of cR_∞, providing an independent check, in a different regime, of the optical measurements. Second is the measurement of the ground state Lamb shift. Because our measurements involve high angular momentum states for which the Lamb shift is extremely small, our results may be compared with optical measurements of transitions between low-lying states to yield an improved measurement of the Lamb shift. Third is to provide a frequency calibration of the spectrum of hydrogen, enabling the creation of a comprehensive frequency standard extending from the radio frequency regime to the ultraviolet.

The experiment employs an atomic beam configuration to reduce Doppler and collisional perturbations. Atomic hydrogen is excited to the low angular momentum n=27 or 29, m=0 state by two-photon stepwise absorption. The excited atoms are then transferred to the longer lived n=27, |m|=26 or n=29, |m|=28 "circular" state by absorption of circularly polarized radio frequency radiation.[3] The atoms enter a region of uniform electric field in which the frequency of the transition (n=27, |m|=26) $\rightarrow$ (n=28, |m|=27) or (n=29, |m|=28) $\rightarrow$ (n=30, |m|=29) is measured by the method of separated oscillatory fields. The final state distribution is analyzed by a state-sensitive electric field ionization detector. The resonance signal appears as a transfer of atoms from the lower state to the upper state as the millimeter-wave frequency is tuned across the transition.

Figure 1 and Figure 2 illustrate the main features of the apparatus. Atomic hydrogen or deuterium is dissociated from H_2 or D_2 in a radio frequency discharge. The beam is cooled by collisions with a cryogenic thermalizing channel in order to slow the atoms and thereby increase the interaction time. After the beam is collimated, the atoms pass through two layers of magnetic shielding and an 80 K cryogenic shield before entering the interaction region. The interaction region is logically divided into three sections: the circular state production region, separated fields region, and detection region. These are described briefly below.

In the circular state production region, the hydrogen atoms are excited from the 1s ground state, through the $2p_{3/2}$ state, to the n=27 or 29, m=0 state by two-photon stepwise excitation. The laser system has been detailed in the 1995 and 1996 *Progress Reports*.[4] The optical excitation is performed in an electric field to provide selective population of a particular m=0 level. The electric field is then rapidly reduced to an intermediate value as the atoms pass through the center of a circle of four electrodes. The antennas are fed by a 1.8 GHz RF source with a 90 degree phase delay between adjacent pairs. This creates a circularly polarized field which drives the atoms into the n=27, |m|=26 or n=29, m=|28| circular state through a multiphoton absorption process. A pulsed electric field ionization (EFI) detector in the circular state production region monitors the efficiency of the optical excitation and angular momentum transfer processes.

After the atoms are prepared in the circular Rydberg state, the beam enters the millimeter-wave separated fields region. Because Rydberg atoms interact strongly with external fields, accurate measurement of the energy level structure requires careful control of the interaction environment. Thermal radiation is reduced by cooling the entire interaction region to $\approx$4 K with a liquid helium flow system. The ambient magnetic field is reduced by the double-wall high-permeablility shields. A small electric field, which defines the quantization axis of the atoms, is applied with high uniformity by field plates above and below the atomic beam. The millimeter-waves intersect the atomic beam at two locations separated by 50 cm. The millimeter-wave optical system was described in the 1990 *Progress Report.*[5] The millimeter-wave zones inside the interaction region, however, have been drastically modified this year and are described below.

3 R. Lutwak, J. Holley, P.P. Chang, S. Paine, D. Kleppner, and T. Ducas, "Circular States of Atomic Hydrogen," *Phys. Rev. A* 56(2): 1443-52 (1997).

4 D. Kleppner et al., *RLE Progress Report* 138: 217 (1995); 139: 209 (1996).

5 D. Kleppner at al., *RLE Progress Report* 133: 145 (1990).

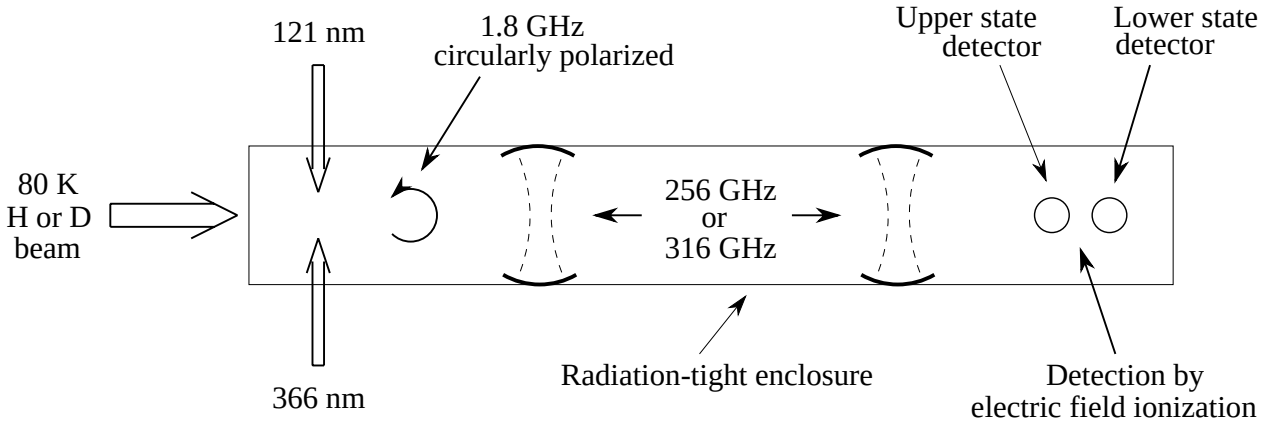

Figure 1. Schematic top view of the apparatus.

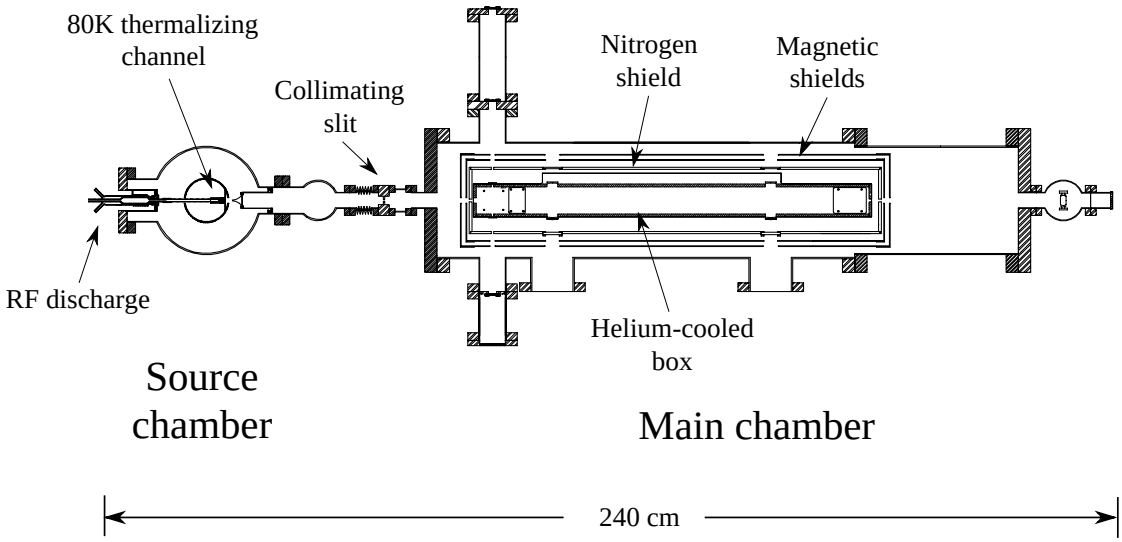

Figure 2. Top view of the atomic beam vacuum apparatus.

The state distribution of the atoms emerging from the interaction region is analyzed by a state-selective electric field ionization detector. Within the detector, the atoms enter a region of increasing electric field produced by a pair of symmetric ramped plates held at constant potential. Atoms in different states are selectively ionized at different fields and the charged nuclei are detected at different positions with two separate electron multipliers. The detection electronics record the state and arrival time of each atom to reach the detector. Because the laser system is pulsed, the time resolution of the ionization signal allows contributions to the resonance pattern from each velocity class to be analyzed individually, providing a valuable check on possible systematic errors.

To find the frequency of the circular state to circular state transition, we measure the population inversion as the millimeter-waves are tuned through resonance. The inversion is defined as

$$\Gamma = \frac{N_{upper} - N_{lower}}{N_{upper} + N_{lower}}$$

where N_{upper} and N_{lower} are the number of ion counts detected in each electron multiplier. As a preliminary diagnostic step, we can leave open only one of the millimeter-wave ports, in which case the resonance curve is a single peak—a "Rabi curve." If both millimeter-wave ports are open, we see the interference fringe characteristic of the Ramsey separated oscillatory fields technique.

This year, we have started to perform millimeter-wave spectroscopy on the n=27 $\rightarrow$ n=28 transition, whereas previously we had confined our efforts to the n=29$\rightarrow$n=30 transition. The two transitions, at 316 GHz and 256 GHz, lie within range of the 5th and 4th harmonics, respectively, of our phase-locked 61-65 GHz Gunn oscillator source. In the past, the extra phase noise on the 5th harmonic had prevented us from observing the 27 $\rightarrow$ 28 resonance, but improvements to our frequency synthesis chain have now made this transition accessible. The 27 $\rightarrow$ 28 transition offers several advantages over the 29 $\rightarrow$ 30 transition, including easier optical excitation to the |m|=0 Rydberg state, a smaller electric field perturbation to the transition frequency, and a fine structure splitting of the resonance line that is 1.5 times larger and hence more easily resolved. A Ramsey interference fringe taken with 80 K deuterium is shown in Figure 3.

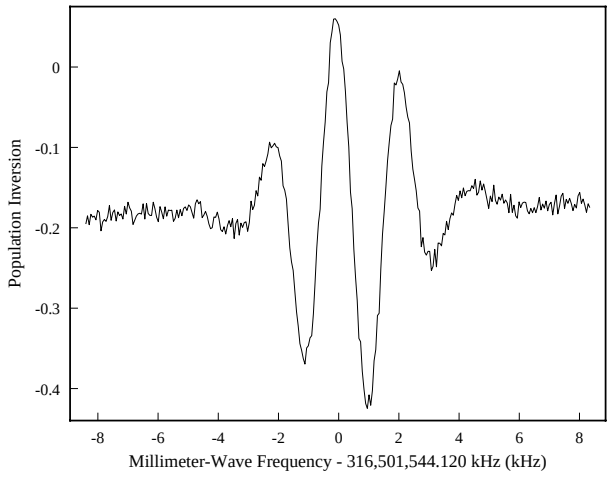

Figure 3. Ramsey interference fringe for the n=27$\rightarrow$n=28 transition in 80 K deuterium.

Because of the asymmetries in the Rabi curves mentioned in last year's *Progress Report*,[6] we have also redesigned the geometry of the millimeter-wave interaction regions. Previously, we used a running wave configuration, with the millimeter-wave beams crossing the atomic beam and then diverted into cold beam dumps inside the helium-cooled enclosure. The asymmetric features in the Rabi curves suggested that a small amount of stray millimeter-wave radiation was not being properly dumped with this geometry. Consequently, we have now gone to a standing wave configuration, employing spherical mirror Fabry-Perot cavities (Figure 4) to contain the millimeter-wave radiation. Each cavity consists of one fixed input coupler mirror and one tunable, completely reflecting, back mirror. The input coupler is fabricated from 500 lines per inch copper mesh epoxied to a quartz substrate. The movable mirror is cut out of solid copper and may be tuned via a mechanical feedthrough on the vacuum chamber. The finesse of the cavities is approximately 400. Each cavity is tuned to a fundamental transverse mode by monitoring the Rabi signal while the longitudinal spacing is varied.

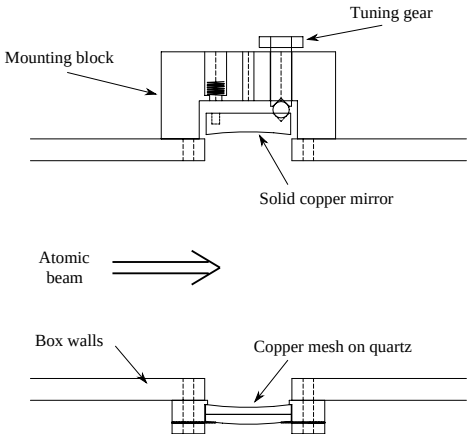

Figure 4. Millimeter-wave interaction zone, including tunable Fabry-Perot cavity.

Figure 5 shows a comparison between running wave and cavity Rabi curves for the n=29$\rightarrow$n=30 deuterium transition. This improvement in the symmetry of the resonance is encouraging, and we expect the accuracy of our Ramsey fringe signal to increase accordingly.

6 D. Kleppner et al., *RLE Progress Report* 138: 217 (1995); 139: 209 (1996).

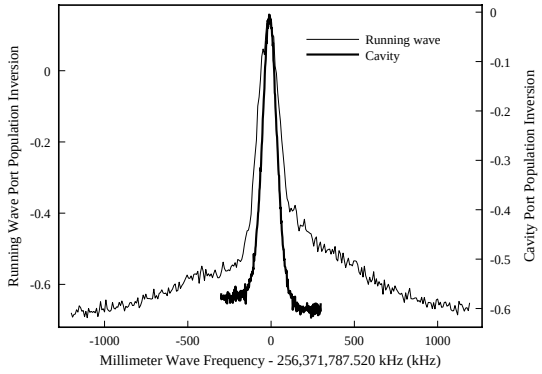

Figure 5. Rabi resonance curves for the n=29 → n=30 transition in 80 K deuterium. Light line: running wave geometry. Dark line: cavity geometry.

2.1.1 Publication

Lutwak, R., J. Holley, P.P. Chang, S. Paine, D. Kleppner, and T. Ducas. "Circular States of Atomic Hydrogen." *Phys. Rev. A* 56(2): 1443-52 (1997).

2.2 Recurrence Spectroscopy of Rydberg Atoms in an Oscillating Field

Sponsors

National Science Foundation
Grant PHY 92-21489
U.S. Navy - Office of Naval Research
Contract N00014-96-1-0484

Project Staff

Neal W. Spellmeyer, Professor Daniel Kleppner

In principle, the classical behavior of a dynamical system can be found from its underlying quantum structure; in practice, general methods do not exist. Rydberg atoms have become prototype systems for the experimental pursuit of the quantum-classical relationship. Experimentally, they exist in the semi-classical regime where such connections should occur, and they can be studied in exquisite detail by laser spectroscopy. Theoretically, much of the phenomena can be interpreted by a variation of Gutzwiller's periodic orbit theory[7] known as closed orbit theory.[8] Closed orbit theory can provide a detailed theoretical descrption of Rydberg atoms in many types of external fields.

Recurrence spectrosopy,[9] a method in which a photoabsorption spectrum is measured under conditions obeying classical scaling laws and then Fourier transformed to yield a "recurrence spectrum," reveals the existence, action, period, and stability of the closed orbits of the classical system. However, there is much more to know about the classical motion—e.g., initial conditions and trajectories. Previously, all studies of recurrence spectra have used static fields. We have taken a new approach by investigating the spectrum of a Rydberg atom in an oscillating field. In collaboration with John B. Delos, M. Haggerty, V. Kondratovich, and J. Gao, we have been able to interpret the spectra quantitatively. Furthermore, we have found how to extract the trajectory of an electron if it propagated classically from quantum spectra.

We study the Rydberg spectrum of lithium in a constant electric field $F = F(\hat{z})$, perturbed with a weak oscillating field $F_1 = F_1\hat{z}\cos(\omega t)$, using cw laser spectroscopy. The experimental setup is similar to that used in an earlier study of recurrence spectra in a static field.[10] The major experimental challenge is to measure and control the oscillating field strength, which we calibrate by measuring sideband structure on a low-lying Rydberg state. While the atoms are in the combined fields, we measure the laser photoexcitation rate from the 3s state to m=0 final states near the field-free ionization limit.

The system can be described by the Hamiltonian for hydrogen because the large-scale structure important to these experiments is unaffected by the lithium core electrons.[11] The Hamiltonian obeys a classical scaling law and can be written

7 M.C. Gutzwiller, *Chaos in Classical and Quantum Mechanics* (Berlin: Springer-Verlag, 1990).

8 M.L. Du and J.B. Delos, "Effect of Closed Classical Orbits on Quantum Spectra: Ionization of Atoms in a Magnetic Field. I. Physical Picture and Calculation," *Phys. Rev. A* 38: 1896 (1988).

9 A. Holle, J. Main, G. Wiebusch, H. Rottke, and K.H. Welge, "Quasi-Landau Spectrum of the Chaotic Diamagnetic Hydrogen Atom," *Phys. Rev. Lett.* 61: 161 (1988).

10 M. Courtney, N. Spellmeyer, H. Jiao, and D. Kleppner, "Classical, Semiclassical, and Quantum Dynamics in the Lithium Stark System," *Phys. Rev. A* 51: 3604 (1995).

$$\tilde{H} = \frac{\tilde{p}^2}{2} - \frac{1}{\tilde{r}} + \tilde{z}\,[1 + \tilde{f}\cos(\tilde{\omega}\tilde{t})] = F^{-\frac{1}{2}}E(t)\ , \qquad (1)$$

where the tildes denote scaled quantities: $\tilde{r} \equiv F^{\frac{1}{2}}r$, $\tilde{p} \equiv F^{-\frac{1}{4}}p$, and $\tilde{t} \equiv F^{\frac{3}{4}}t$.[12] Because of the scaling law, the classical dynamics depends only on three parameters: the scaled energy $\varepsilon \equiv E_0F^{-1/2}$($E_0$ is the initial energy of the electron), the scaled field strength $\tilde{f} \equiv F_1/F$, and the scaled frequency $\tilde{\omega} \equiv \omega F^{-3/4}$.

We measure scaled spectra by recording the photoabsorption spectrum as a function of $w \equiv F^{-1/4}$ while the laser energy, the static and rf field amplitudes (we use "rf" to refer to a field whose frequency may extend into the microwave regime), and the rf frequency are varied simultaneously so as to maintain ε, $\tilde{f}$, and $\tilde{\omega}$ constant. The magnitude squared of the Fourier transform of a scaled spectrum with respect to w is the recurrence spectrum. Examples of recurrence spectra in an oscillating field are shown in Figures 6 and 8.

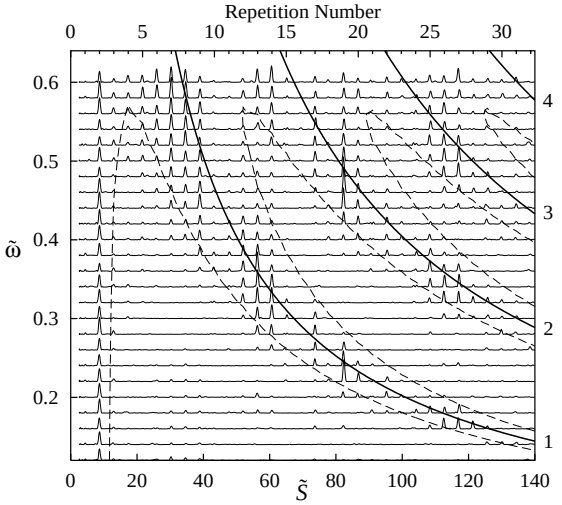

Figure 6. Experimental recurrence spectra recorded at $\varepsilon = -0.4$ and $\tilde{f}$ = 0.005, with scaled frequency $\tilde{\omega}$ between 0.12 and 0.60. The dashed lines are contours generated from an approximate form of closed orbit theory that mark regions in which recurrences should remain strong.

Closed orbit theory provides a physical picture and analytical description of static field recurrence spectra, and has been extended to describe our results in the oscillating field. The laser radiation produces a stream of outgoing waves which, in the semiclassical approximation, follow classical trajectories. As the trajectories travel outward, some are turned back by the combined Coulomb and applied fields and return to the nucleus. These interfere with the outgoing waves (and with each other), giving rise to oscillatory patterns in the absorption spectrum. Each returning orbit k gives a sinusoidal contribution to the oscillator strength density[13],

$$Df_{1,\kappa}(\varepsilon, w) = C_\kappa \sin[\tilde{S}^0_\kappa(\varepsilon)w + \lambda\kappa]\ . \qquad (2)$$

$\tilde{S}^0_\kappa(E, F) \equiv \int \tilde{p}\cdot d\tilde{q}$ is the classical action around the closed orbit, $w = F^{-1/4}$, and λ_κ is a phase correction associated with Maslov indices. C_κ is the recurrence amplitude, which is approximately independent of w. The recurrence spectra reveal peaks at $\tilde{S}$ with strengths $|C_k|^2$.

As explained in Spellmeyer,[14] closed orbit theory describes recurrence spectra in a weak oscillating field with a similar physical picture. For each closed orbit in the time-independent system, there is a continuous manifold of orbits whose properties depend on the relative phase between the launch of an orbit and the phase of the field. Closed orbit theory incorporates these orbits by generalizing (2) to include an average over all phases. In the limit that the oscillating field is weak, it can be shown[15] that (2) becomes

$$Df_{1,\kappa} = C_\kappa J_0(\tilde{f}\left|\tilde{Z}_\kappa(\tilde{\omega})\right|\tilde{T}_k w)\sin[\tilde{S}^0_\kappa(\varepsilon)w + \lambda\kappa] \qquad (3)$$

$\tilde{T}_\kappa$ is the period of the *unperturbed* orbit, and $\tilde{Z}_k(\omega)$ is the time-averaged ac dipole moment of the *unperturbed* orbit, $(1/T_k)\int_0^{T_k} z(\tau)z(\tau)e^{-\omega\tau}d\tau$. This result provides a general description of the absorption spectrum of a Rydberg atom in a weak oscillating electric field. The recurrence strength associated with orbit k is reduced by the factor

11 M. Courtney, N. Spellmeyer, H. Jiao, and D. Kleppner, "Classical, Semiclassical, and Quantum Dynamics in the Lithium Stark System," *Phys. Rev. A* 51: 3604 (1995).

12 N. Spellmeyer, D. Kleppner, M.R. Haggerty, V. Kondratovich, J.B. Delos, and J. Gao, "Recurrence Spectroscopy of a Time-Dependent System: A Rydberg Atom in an Oscillating Field," *Phys. Rev. Lett.* 79: 1650 (1997).

13 V. Kondratovich and J.B. Delos, "Scaled-energy Floquet Spectroscopy in a Strong Electric Field: A Semiquantal Calculation of the Recurrence Spectrum," submitted to *Phys. Rev. A.*

$$a_k(\tilde{f}) \equiv J_0^2(\tilde{f}T_k\left|\tilde{Z}_k(\tilde{\omega})\right|w) \quad (4)$$

where w is given by the average value of $F^{-1/4}$.

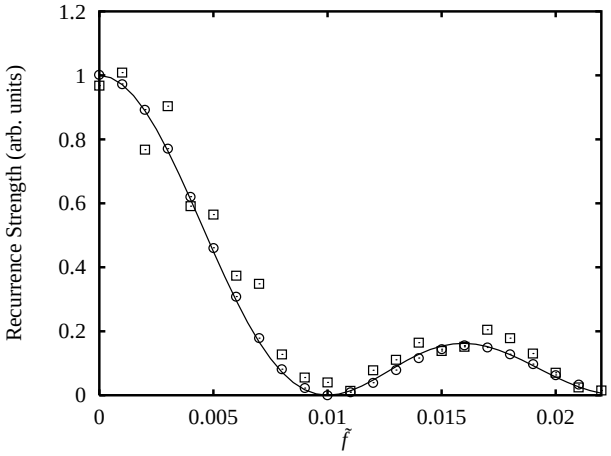

Figure 7. Recurrence strength of the second repetition at $\varepsilon = -0.4$ and $\tilde{\omega}=0.32$ versus $\tilde{f}$. Squares are experimental recurrence strengths, circles are from Floquet computa-tions. The solid line is the prediction of closed orbit theory.

This formula has been tested on spectra including those shown in Figure 6. The results show good agreement with the experiments and with "semiquantal" Floquet computations of the spectra.[16] As an example, Figure 7 shows the strength of the recurrence at the action of the second repetition of the uphill parallel orbit.

We have used this new type of spectroscopy in a series of experiments in which we have measured with finite time-resolution the z(t) components of the classical trajectories of two orbits important in the Stark system.[17] We measure recurrence spectra at a series of increasing values of $\tilde{f}$, at a fixed frequency $\tilde{\omega}$ (see Figure 8) and extract the ac dipole moment of the orbit by fitting to theory. We then find z(t) by inverse Fourier transforming the measured ac dipole moment over the experimental frequency range.

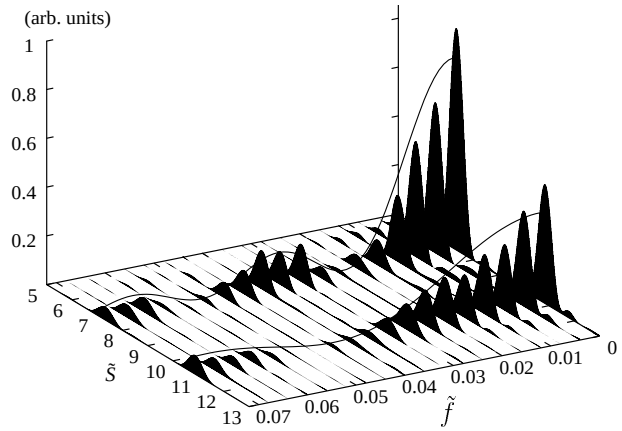

Figure 8. Experimental recurrence spectra in an oscil-lating electric field, $\varepsilon = -2.05$, $\tilde{\omega} = 1.4$. The recurrences at $\tilde{S}$ = 7.23 correspond to the 2/3 orbit, those at $\tilde{S}$ = 10.68 to the 3/4 orbit. The lines are fits of the data to Eq.(4).

A major difficulty is the loss of the complex phase of $\tilde{Z}_k(\omega)$. Physically, this phase indicates when the electron left the atom relative to the phase of the field. Fortunately, it is possible to recover the phase in our system because all of the closed orbits in a static electric field are time-reversal symmetric. For orbits with this symmetry, it can be shown that $\tilde{Z}_\kappa(\tilde{\omega})$ can be found from its magnitude if an orbit's static dipole moment, $\tilde{Z}_k(\omega)$, is known. This quantity can in turn be found from the period of the orbit, which we measure using recurrence spectroscopy. After the phase has been reconstructed, we invert the measured ac dipole moment $\tilde{Z}_k\tilde{\omega}$ by expressing it as a sum of smooth basis functions and fitting to the data to find the trajectory $\tilde{z}_k(\tau)$.

We have studied two closed orbits of lithium, the "2/3" and the "3/4" orbits.[18] Figure 8 shows the recurrences corresponding to these orbits at a single value of $\tilde{\omega}$ and a range of values of $\tilde{f}$. Seventeen such series of measurements were made in the

14 N. Spellmeyer, D. Kleppner, M.R. Haggerty, V. Kondratovich, J.B. Delos, and J. Gao, "Recurrence Spectroscopy of a Time-Dependent System: A Rydberg Atom in an Oscillating Field," *Phys. Rev. Lett.* 79: 1650 (1997).

15 Ibid.

16 V. Kondratovich and J.B. Delos, "Scaled-energy Floquet Spectroscopy in a Strong Electric Field: A Semiquantal Calculation of the Recurrence Spectrum," submitted to *Phys. Rev. A.*

17 M.R. Haggerty, J.B. Delos, N. Spellmeyer, and D. Kleppner, "Extracting Classical Trajectories from Atomic Spectra," submitted to *Phys. Rev. Lett.*

range $0.6 \le \tilde{\omega} \le 4.0$. The resulting values of $\tilde{T}_\kappa \left| \tilde{Z}_\kappa \right|$ for the 2/3 and 3/4 orbits are shown in Figure 9. It can be seen that across the experimentally accessible frequency range, agreement between data and theory is good within about 10%.

.

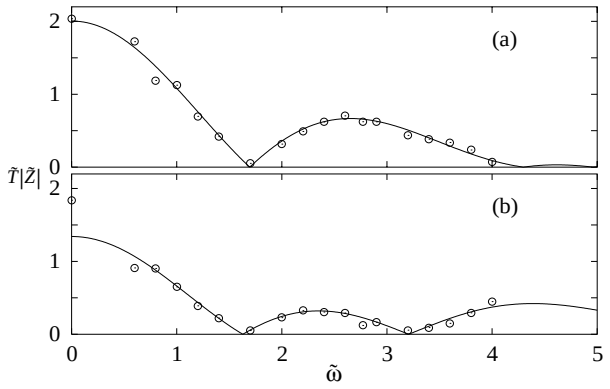

Figure 9. Experimental measurement of $\tilde{T}\left|\tilde{Z}\tilde{\omega}\right|$. Circles are experimental measurement. Lines are classical calculation. (a) 2/3 orbit; (b) 3/4 orbit.

Figure 10 shows $\tilde{z}(\tau)$ for the two trajectories. The heavy solid line shows the orbits as reconstructed by this experiment. The dashed line shows the result doing the inversion using exact classical calculations windowed over the experimental frequency range. The light solid lines are the exact classical trajectories. Although our time-resolution is limited by the limited frequency range of the experiment, we are able to resolve many features of the classical motion. Both orbits initially move from the nucleus in the –z direction before they are turned back toward the nucleus by the electric field. The 2/3 orbit loops back to the nucleus once before closing while the 3/4 loops back twice. These features of the classical motion could not be studied previously to this work. It can be shown that features could be measured with much higher resolution before being limited by the uncertainty principle and the breakdown of the semi-classical limit.

In summary, we have developed a new type of recurrence spectroscopy in which information about classical motion at a given frequency can be measured. Experiments show good agreement with a version of closed orbit theory developed in response to the measurements, and also with Floquet computations of the spectra. We have applied this technique to measure with finite resolution the classical trajectories of two orbits in the Stark system. The technique promises to serve as a new method for extracting classical motion from quantum spectra.

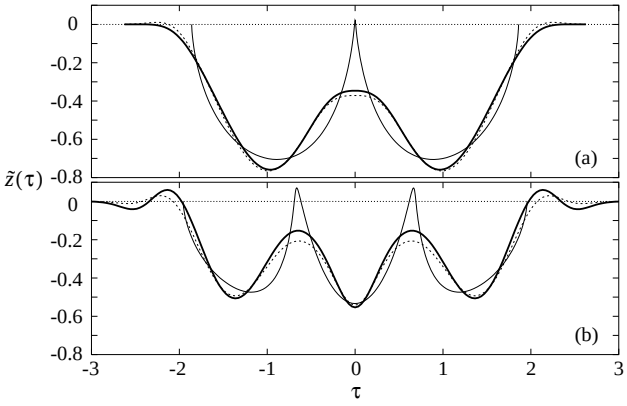

Figure 10. Reconstruction of classical orbits. The light solid lines show the exact classical trajectory $\tilde{z}(\tau)$ for the orbit. The heavy solid line shows the result of the experimental measurement. The dashed lines show the result of an exact reconstruction of the orbit, filtered to include Fourier components in the experimental range $0 \le \tilde{\omega} \le 4.0$. (a) 2/3 orbit; (b) 3/4 orbit.

2.2.1 Publications

Haggerty, M.R., J.B. Delos, N. Spellmeyer, and D. Kleppner. "Extracting Classical Trajectories from Atomic Spectra." Submitted to *Phys. Rev. Lett.*

Spellmeyer, N., D. Kleppner, M.R. Haggerty, V. Kondratovich, J.B. Delos, and J. Gao. "Recurrence Spectroscopy of a Time-Dependent System: A Rydberg Atom in an Oscillating Field." *Phys. Rev. Lett.* 79: 1650 (1997).

Thesis

Spellmeyer, N. *Rydberg Atoms in an Oscillating Field: Extracting Classical Motion from Quantum Spectra.* Ph.D. diss., Department of Physics, MIT, 1998.

18 J. Gao and J.B. Delos, "Resonances and Recurrences in the Absorption Spectrum of an Atom in an Electric Field," *Phys. Rev. A* 49: 869 (1994).

2.3 Atom Interferometry

Sponsors

Joint Services Electronics Program
Grant DAAH04-95-1-0038
National Science Foundation
Grant PHY95-14795
U.S. Army Research Office
Contract DAAH04-94-G-0170
Contract DAAG55-97-1-0236
Contract DAAH04-95-1-0533
U.S. Navy - Office of Naval Research
Contract N00014-96-1-0432

Project Staff

Edward T. Smith, Richard A. Rubenstein, David A. Kokorowski, Tony Roberts, Huan Yao, Dr. Al-Amin Dhirani, Professor David E. Pritchard

Atom interferometers, in which atom or molecule deBroglie waves are coherently split and then recombined to produce interference fringes, have opened exciting new possibilities for precision and fundamental measurements with complex particles. The ability to accurately measure interactions that displace the deBroglie wave phase has led to qualitatively new measurements in atomic and molecular physics, fundamental tests of quantum mechanics, and new ways to measure acceleration and rotation:

- Atom interferometers allow us to make completely new investigations of atoms and molecules including precision measurements of atomic polarizabilities that test atomic structure models, determination of long range forces important in cold collisions and Bose-Einstein condensation, and measurements of molecular polarizability tensor components.
- Atom interferometers allow us to make fundamental investigations in quantum mechanics. These include measurements of topological and geometric phases, loss of coherence from a quantum system, quantum measurement, and investigations of multi-particle interferometry and entanglement.
- The large mass and low velocities of atoms makes atom interferometers especially useful in inertial sensing applications, both as precision accelerometers and as gyroscopes. They have a potential sensitivity to rotations ~10^{10} greater than optical interferometers of the same area.
- Atom interferometers may have significant applications to condensed matter physics, including measurements of atom-surface interactions and lithography using coherently manipulated fringe patterns that are directly deposited onto substrates.
- Longitudinal atom interferometers are easily capable of measuring phase shifts due to velocity changes of 1 part in 10^{10}.

Our group has pioneered many of these areas, including the first (and only) atom interferometry experiments that employ physically separated paths with different interactions on each. These investigations have proved to be of wide-spread general interest to the scientific community and have received notice in the popular scientific press.[19]

During 1997, we made significant progress towards our long term goal of developing further applications and expanding the intrinsic capabilities of atom interferometers. In particular, we (1) published a paper demonstrating for the first time the remarkable sensitivity of atom interferometers to rotation sensing,[20] (2) developed the theory[21] and experimental techniques[22] for a longitudinal atom interferometer, and (3) have substantially improved our apparatus.

19 Articles on recent work performed by our interferometer group have appeared in various publications including: P.F. Schewe and B. Stein, *AIP Phys. Bull. Phys. News,* Jan. 4, 1996; T. Sudbery, *Nature* 379: 403 (1996); J. Hecht, *Laser Focus World* 32: 20 (1996); D.H. Freedman, *Discover* 17: 58 (1996); *Physics Today* 50: 9 (1997); C. Seife, *Sci.* 275: 931 (1997); P. Yam, Sci. Am. 276(6): 124 (1997); R. Pool, *Discover* 18:103 (1997); M. Browne, "It's a Molecule. No, It's More Like a Wave," *NY Times* (Science Section) August 15, 1995.

20 A. Lenef, T.D. Hammond, E.T. Smith, M.S. Chapman, R.A. Rubenstein, and D.E. Pritchard, "Rotation Sensing with an Atom Interferometer," *Phys. Rev. Lett.* 78: 760 (1997).

21 D.E. Pritchard, R.A. Rubenstein, A. Dhirani, D.A. Kokorowski, T.D. Hammond, B. Rohwedder, and E.T. Smith, forthcoming.

22 E.T. Smith, A. Dhirani, D.A. Kokorowski, R.A. Rubenstein, T.D. Roberts, H. Yao, and D.E. Pritchard, forthcoming.

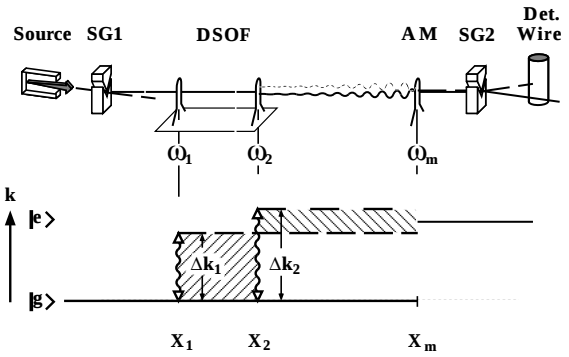

Figure 11. (Top) A schematic view of the apparatus. Hair-pin coils at longitudinal positions x_1 and x_2 with oscillatory fields at ω_1 and ω_2, respectively, constitute the DSOF region. The amplitude modulator coil is located at x_m. The initial (ground) state is selected by upstream Stern-Gerlach magnet SG1, and the final (excited) state by SG2. (Bottom) Wavenumber, k, versus the position, x, for states that are overlapped and detected in the longitudinal interferometer. Detuned transitions between the ground and excited internal states give rise to wavenumber changes Δk_1 and Δk_2 at the first and second DSOF coils, respectively. Left (right) hatched area denotes the differential phases accrued by molecules excited at x_1 and x_2.

2.3.1 Longitudinal Atom Interferometry

The central idea of atom interferometry is that each atom's deBroglie wave is split and sent over different "paths" with resulting interference fringes where it is recombined. Generally, the two paths differ in the direction of the waves, but not the wavelength (except for some difference in the local interactions, as we have demonstrated in our "transverse" atom interferometer). However, one may also envision placing each atom's wave in a superposition involving different wavelengths corresponding to different longitudinal momenta (and energy). Over the past year, we have developed a theory showing that resonance regions can create and recombine such longitudinal momentum coherences, basically serving as atomic beam splitters. By taking full advantage of the freedom to apply different frequencies to successive oscillatory field regions—termed DSOF, a generalization of Ramsey's separated oscillatory field method—we have demonstrated a "white fringe" longitudinal interferometer capable of generating, rephasing, and detecting coherences dephased because atoms with different velocities accumulate different phases. Several new applications of longitudinal interferometry are described below.

2.3.2 Improvements to the Apparatus

We are continuing to make several important improvements to our apparatus. Collaborating with Professor Henry I. Smith's group at MIT to fabricate improved atom transmission gratings using holographic lithography, we have demonstrated atom interference fringes (unfortunately with low contrast) using 100 nm period gratings. These gratings give twice the beam separation of our standard 200 nm gratings. We have also significantly upgraded our apparatus. The separated beam atom optical elements have been placed on an optical platform separate from the vacuum envelop which should substantially improve the flexibility of the interferometer as well as its thermal and vibration isolation. The vacuum envelop itself has been replaced by a series of standard six-way crosses, achieving greater length, facilitating access to the equipment inside the chamber, and permitting the rapid reconfiguration of modular flanges which currently hold the atom optical elements for our longitudinal interferometer. The new apparatus should be very stable and allow the simultaneous pursuit of several different experiments.

2.3.3 Ongoing Investigations

Longitudinal interferometry**:** The extension of atom interferometry to include longitudinal coherences represents an exciting frontier. We are currently using the DSOF geometry to measure the longitudinal momentum density matrix of a molecular beam, thereby resolving a longstanding controversy concerning the longitudinal momentum structure of atomic beams.[23] The extraordinary sensitivity of longitudinal interferometers to differential changes in vel-ocity of the atom beam can be exploited to detect very small forces. An example is the controversial Anandan force that acts differentially on the components of the wavefunction on opposite legs of a separated atomic beam interferometer.[24] Finally, the tech-

23 A. Dhirani, D.A. Kokorowski, R.A. Rubenstein, T.D. Hammond. B. Rohwedder, E.T. Smith, A.D. Roberts and D.E. Pritchard, "Determining the Density Matrix of a Molecular Beam using a Longitudinal Matter Wave interferometer," *J. Mod. Opt.* 44(11/12): 2583 (1997).

24 J. Anandan, *Phys. Rev. Lett.* 48: 1660 (1982).

niques developed here will permit us to implement a velocity multiplexing scheme for the precision measurement of large interferometric phase shifts.[25]

Velocity dependent index of refraction: The physical separation of beam paths in our transverse interferometer permits both amplitude and phase changes in the interference pattern to be observed as one of the interfering atom beams is exposed to some interaction. Using this capability, we recently performed an experiment measuring the index of refraction of various gases and hence the role of atom-atom interactions in collisions.[26] We are planning to extend this experiment to probe for velocity dependencies. There is significant interest in the theoretical community in such results as the interactions are determined by the long range behavior of the atomic potentials; for example, it is predicted that the index of refraction should exhibit Glory oscillations as the velocity of the impinging gas is varied.

Quantum decoherence: Scattering photons from atoms while they are inside an interferometer causes the atoms to change their state. We believe that under suitable conditions, this will not destroy the quantum coherence but rather will cause the atoms to diffuse in momentum space. This experiment is significant since it generalizes our recent realization of Feynman's *gedanken* experiment[27] in which decoherence from single photon scattering was measured and then recovered. Also, quantum decoherence is just becoming accessible to study as an important experimental barrier to constructing quantum computers.

Geometric Phases: Precision measurements of the Aharonov-Casher (AC) phase are planned. These will allow a study of the dependence on the interfering particle's dipole orientation for the first time. Modifications made to our interaction region (a device which allows different potentials to be applied to either arm of the interferometer) to introduce spatially varying magnetic fields will permit investigations of Berry's phase as well.

2.3.4 Publications

Dhirani, A., D.A. Kokorowski, R.A. Rubenstein, T.D. Hammond. B. Rohwedder, E.T. Smith, A.D. Roberts and D.E. Pritchard. "Determining the Density Matrix of a Molecular Beam using a Longitudinal Matter Wave interferometer." *J. Mod. Opt.* 44(11/12): 2583 (1997).

Lenef, A., T.D. Hammond, E.T. Smith, M.S. Chapman, R.A. Rubenstein, and D.E. Pritchard. "Rotation Sensing with an Atom Interferometer." *Phys. Rev. Lett.* 78: 760 (1997).

Pritchard, D.E., R.A. Rubenstein, A. Dhirani, D.A. Kokorowski, T.D. Hammond, B. Rohwedder, and E.T. Smith. "Fully Quantized Treatment of Molecular Beam Resonance: Momentum Coherences and Entanglements." To be submitted.

Smith, E.T., A. Dhirani, D.A. Kokorowski, R.A. Rubenstein, T.D. Roberts, H. Yao, and D.E. Pritchard. "Velocity Rephased Longitudinal Momentum Coherences with Differentially Detuned Separated Oscillatory Fields." *Phys. Rev. Lett.* Forthcoming.

Thesis

Hammond, T.D. *Atom Interferometry: Dispersive Index of Defraction and Rotation Induced Phase Shifts for Matter Waves.* Ph.D. diss., Department of Physics, MIT, 1997.

2.4 Precision Mass Spectrometry of Ions

Sponsors

Joint Services Electronics Program
Grant DAAH04-95-1-0038
National Science Foundation
Contract PHY92-22768

Project Staff

Michael P. Bradley, Simon Rainville, James R. Thompson, Roland N. Nguyen, Dr. James V. Porto, Professor David E. Pritchard

25 T.D. Hammond, D.E. Pritchard, M.S. Chapman, A. Lenef, and J. Schmiedmayer, *App. Phys. B* 60: 193 (1995); T.D. Hammond, Ph.D. diss., Department of Physics, MIT, 1997.

26 J. Schmiedmayer, M.S. Chapman, C.R. Ekstrom, T.D. Hammond, S. Wehinger, and D.E. Pritchard, "Index of Refraction of Various Gases for Sodium Matter Waves," *Phys. Rev. Lett.* 74: 1043 (1995).

27 M.S. Chapman, T.D. Hammond, A. Lenef, J. Schmiedmayer, R.A. Rubenstein, E.T. Smith, and D.E. Pritchard, "Photon Scattering from Atoms in an Atom Interferometer: Coherence Lost and Regained," *Phys. Rev. Lett.* 75: 3783 (1995); R. Feynman, R. Leighton, and M. Sands, *The Feynman Lecture Notes,* Vol. III (Reading, Mass.: Addison-Wesley, 1966).

2.4.1 Overview

We have recently published two papers[28] which firmly establish our measurements of atomic mass as the most accurate in the world. Our mass table consists of ten atomic masses of particular importance to physics or metrology.[29] The accuracy of these masses, typically 10^{-10}, represents one to three orders of magnitude improvement over previously accepted values. These results represent important contributions in both fundamental physics and metrology, including:

- 80-fold improvement of the current x-ray wavelength standard by using $E = \Delta m\, c^2$ to determine the energies of gamma rays from neutron capture by ^{14}N (which are widely used as gamma ray calibration lines) from a measurement of the associated mass difference.
- Our accurate determination of the atomic weight of ^{28}Si opens the way for an atomic standard of mass by replacing the "artifact" kilogram mass standard with a crystal of pure silicon.

2.4.2 Recent Progress

In 1997, we made a number of improvements to our single ion Penning trap and detector so that in 1998 we will be able to make a variety of important measurements. These will enable us to (1) increase the number of different masses measured and (2) increase the accuracy of the masses we have already measured by an order of magnitude.

Measurements of immediate interest to us include:

- Determination of the molar Planck constant, $N_A h$, by measuring the atomic mass and recoil velocity of a Cs atom that has absorbed a photon of known wavelength. Our upcoming measurement of the mass of Cs, combined with ongoing experiments in Chu's lab at Stanford should provide a direct measurement of $N_A h$ to an accuracy near 10^{-9}, leading to a determination of the fine structure constant at 6×10^{-10} which will check the QED value.
- Measurement of the ^3H - ^3He mass difference, which is important in ongoing experiments to determine the electron neutrino rest mass.

The improvements that will allow us to make these measurements include methods for loading a wider variety of ions into the trap, improvements to the ion detector and improving the hardware and software for directly controlling the amplitude and phase of a single ion's magnetron orbits. Using the new loading technique we have demonstrated the ability to produce, trap and detect triply charged Cs ions. We have upgraded our single ion detector, replacing the rf squid with a much quieter dc squid, and developing better superconducting coupling resonators that increase the quality factor of our detector to Q = 50,000.

With these improvements, we have demonstrated that the new detector has at least a factor of 10 less instrumental noise. We can now circumvent some of the limitations due to thermal noise in the coupling circuit, the dominant source of noise in the system, and may be able to measure and remove the 4K thermal motion of the ion. The recent changes, along with the demonstration of a squeezing technique to reduce the relativistic shifts due to thermal noise, make it possible for another dramatic improvement in mass resolution to be obtained by comparing two ions trapped in the same field. This will allow:

- Checking the relationship $E = mc^2$ to a part in 10^7 by weighing neutron capture γ-rays of silicon, sulfur, or chlorine whose wavelengths will be measured by a NIST group; this will also provide an independent determination of $N_A h$ and the fine structure constant;
- Determination of excitation and binding energies of atomic and molecular ions by weighing the associated small decrease in mass, $\Delta m = E_{bind}/c^2$ (we must reach our ultimate goal of a few times 10^{12} to make this a generally useful technique);
- Improvement of some traditional applications of mass spectrometry resulting from our orders of magnitude improvement in both accuracy and sensitivity.

We achieve this accuracy by measuring the cyclotron resonance of a single molecular or atomic ion in a Penning trap, a highly uniform magnetic field in which

28 F. DiFilippo, V. Natarajan, M. Bradley, F. Palmer, and D.E. Pritchard, *Physica Scripta T59:* 144-54 (1995); F. DiFilippo, V. Natarajan, M. Bradley, F. Palmer, and D.E. Pritchard, in *Atomic Physics 14,* (New York: American Institute of Physics Press, 1995).

29 F. DiFilippo, V. Natarajan, K. Boyce, and D.E. Pritchard, *Phys. Rev. Lett. 73*: 1481 (1994).

confinement along the magnetic field lines is provided by much weaker electric fields. We monitor the ion's axial oscillation by detecting the tiny currents induced in the trap electrodes—the current induced by a single ion can be as small as 10^{-15} amps. Measuring such a current requires an extremely sensitive detector, and we are fortunate to have improved the ultrasensitive superconducting electronics we developed for this application.[30] This work in trapping and precision resonance draws on techniques developed by Dr. Hans Dehmelt at the University of Washington and Dr. Norman Ramsey at Harvard, for which they shared in the 1989 Nobel Prize.

We have developed techniques for driving, cooling, and measuring the frequencies of the three normal modes of ion motion in a Penning trap. Thus, we can manipulate the ion position reproducibly to within 30 microns from the center of the trap, correcting for electrostatic shifts in the cyclotron frequency to great accuracy. We use a π-pulse method to coherently swap the phase and action of the cyclotron and axial modes.[31] Therefore, although we detect only the axial motion directly, we can determine cyclotron frequency by measuring the phase accumulated in the cyclotron motion in a known time interval. We can measure the phase of the cyclotron motion to within 10 degrees, leading to a precision of 10^{-10} for a one-minute measurement. Our entire ion-making process is fully automated, and the computer can cycle from an empty trap to having a cooled single ion in about three minutes under optimal conditions.

The typical statistical fluctuation in our magnetic field limits our overall accuracy to at best 8 x 10^{-11} (see Figure 12). While this is a significant accomplishment, we have made major advances toward our long term goal of improving our accuracy by more than one additional order of magnitude. This will be achieved by measuring the cyclotron frequencies of two ions trapped in the same field at the same time to eliminate the problem of field fluctuations and by using squeezing techniques to reduce thermal noise. We have modified our apparatus to allow excitation and detection of two ions at the same time and demonstrated the capability of two ion measurements to reduce the effects of field fluctuations; however, expansion of our previous theoretical understanding[32] of two ion dynamics to include the effects of minute imperfections in the trapping fields has led us to the conclusion that it will not be possible to place two ions in the same trap at one time.

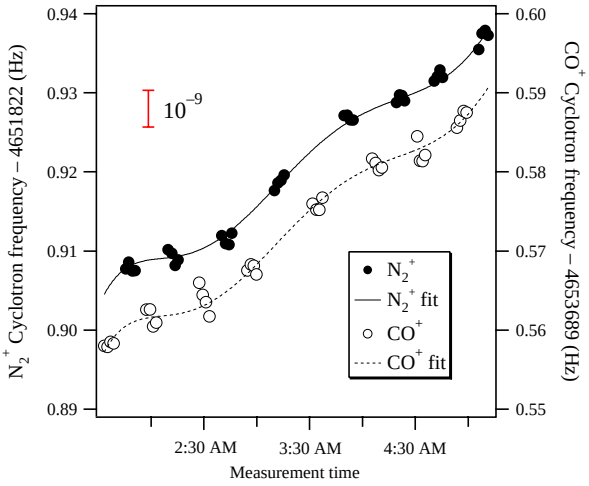

Figure 12. Cyclotron frequency as a function of time for alternate N_2^+ and CO^+ ions in our Penning trap. The fre-quencies are obtained after a 50s integration of cyclotron phase (see text). The solid line is a polynomial fit to the drift in the field common to both ions.

We are therefore pursuing a second method for overcoming the limits due to magnetic field fluctuations: placing two ions in closely adjacent traps. We have investigated and modeled methods for swapping the ions between the two traps, evaluated the leading sources of error, and designed an arrangement of superconducting coils that will prevent the magnetic fields in the two traps from fluctuating independently. We have machined a special “double trap” which consists of two Penning traps axially aligned with each other. This project is very promising, because even if we run into unexpected problems simultaneously detecting two ions in separate traps, we can use one of the traps as a “holding tank” for the ion of a pair which is not being measured. This would significantly decrease the time between measurements and could increase the rate of measurement by as much as a factor of four, decreasing our statistical uncertainty by a factor of 2. The holding tank would

30 R. Weisskoff, G. Lafyatis, K. Boyce, E. Cornell, R. Flanagan, Jr., and D.E. Pritchard, *J. Appl. Phys.* 63*:* 4599 (1988).

31 E.A. Cornell, R.M. Weisskoff, K. Boyce, and D.E. Pritchard, *Phys. Rev. A* 41: 312 (1992).

32 E.A. Cornell, K. Boyce, D.L.K. Fygenson, and D.E. Pritchard, *Phys. Rev. A 45:* 3049 (1992).

also be useful for measurements of radioactive ions such as ^{3}H, since it would dramatically decrease the buildup of radioactive material on the trap electrodes.

With either two-ion scheme, the primary source of measurement noise will be the special relativistic mass shift due to thermal fluctuations in cyclotron amplitude. We have proposed several methods of classical squeezing with parametric drives to reduce amplitude fluctuations[33] and demonstrated the simplest of these,[34] reducing the effects of thermal noise by about a factor of two. In addition, with our new detector, we should be able to surpass limitations due to thermal noise power in our coupling circuit by tuning the ion's resonance away from the detector resonance.

2.4.3 Publication

Bradley, M., F. Palmer, D. Garrison, L. Ilich, S. Rusinkiewicz, and D.E. Pritchard. "Accurate Mass Spectrometry of Trapped Ions." *Hyperfine Interact. 108:* 227-38 (1997).

2.5 Cooling and Trapping Neutral Atoms

Sponsors

David and Lucile Packard Foundation
Grant 96-5158
National Science Foundation
Grant PHY 95-01984
U.S. Army Research Office
U.S. Navy - Office of Naval Research
Contract N00014-96-1-0485
AASERT N00014-94-1-0807

Project Staff

Professor Wolfgang Ketterle, Dr. Hans-Joachim Miesner, Dr. Chandra S. Raman, Dr. Jörn Stenger, Dr. Christopher G. Townsend, Roberto Onofrio, Michael R. Andrews, Ananth P. Chikkatur, Dallin S. Durfee, Shin Inouye, Christopher E. Kuklewicz, Dan M. Stamper-Kurn, Johnny M. Vogels

2.5.1 Introduction

The observation of Bose-Einstein condensation (BEC) in dilute atomic gases[35] was the realization of many long-standing goals: (1) to cool neutral atoms into the ground state of the system, thus exerting ultimate control over the motion and position of atoms limited only by Heisenberg's uncertainty relation; (2) to generate a coherent sample of atoms all occupying the same quantum state (this was subsequently used to realize an atom laser, a device which generates coherent matter waves); and (3) to create a quantum fluid with properties quite different from the quantum liquids He-3 and He-4. This provides a test ground for many-body theories of the dilute Bose gas which were developed many decades ago, but never tested experimentally. Bose-Einstein condensates offer intriguing possibilities for further research. They are predicted to show superfluidity and other manifestations of coherent behavior and are likely to find use in a variety of applications, e.g., atom interferometry, precision measurements, and atom optics.

Our major advances in 1997 were (1) the realization of an all-optical trap for Bose-Einstein condensates which eliminates many restrictions of the magnetic traps used so far for further studies of atom lasers and Bose-Einstein condensates, (2) a detailed study of sound propagation and collective excitations in Bose-Einstein condensates, and (3) a study of the formation process of the condensate, which is based on "matter wave amplification" and provides the gain process for an atom laser.

2.5.2 All-optical Confinement of a Bose-Einstein Condensate

Magnetic confinement of Bose-Einstein condensates is incompatible with many precision measurements and applications in atom optics. We have realized an optical trap for a Bose-Einstein conden-

33 F. DiFilippo, V. Natarajan, K. Boyce, and D.E. Pritchard, *Phys. Rev. Lett. 68:* 2859 (1992).

34 V. Natarajan, F. DiFilippo, and D.E. Pritchard, *Phys. Rev. Lett.74:* 2855 (1995).

35 M.H. Anderson, J.R. Ensher, M.R. Matthews, C.E. Wieman, and E.A. Cornell, "Observation of Bose-Einstein Condensation in a Dilute Atomic Vapor," *Sci.* 269: 198 (1995); K.B. Davis, M.-O. Mewes, M.R. Andrews, N.J. van Druten, D.S. Durfee, D.M. Kurn, and W. Ketterle, "Bose-Einstein Condensation in a Gas of Sodium Atoms," *Phys. Rev. Lett.* 75: 3969 (1995); C.C. Bradley, C.A. Sackett, and R.G. Hulet, "Bose-Einstein Condensation of Lithium: Observation of Limited Condensate Number," *Phys. Rev. Lett.* 78: 985 (1997), see also: C.C. Bradley, C.A. Sackett, J.J. Tollet, and R.G. Hulet, "Evidence of Bose-Einstein Condensation in an Atomic Gas with Attractive Interactions," *Phys. Rev. Lett.* 75: 1687 (1995).

sate.[36] It uses a single focused infrared laser beam of only a few milliwatts of laser power, which is sufficient due to the very low energy of Bose condensates. In this trap, we have observed high atomic densities which were unprecedented both for Bose condensates and optically trapped atoms. Furthermore, the trap works at arbitrary magnetic fields and for atoms in all hyperfine states. Simultaneous confinement of Bose-Einstein condensates in several hyperfine states was demonstrated (see Figure 13) and can be used to study multicomponent condensates. Finally, the optical trap may also serve as an "optical tweezers" to move condensates and, for example, place them in optical and microwave cavities close to surfaces.

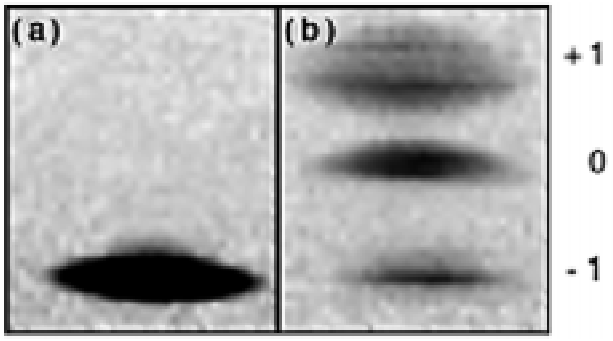

Figure 13. Optical trapping of condensates in all F = 1 hyperfine states. Shown are absorption images of ballistically expanding condensates after switching off the optical trap. Hyperfine states were separated by a magnetic field gradient pulse during the 40 msec time-of-flight. Atoms remained spin-polarized ($m = -1$ state) in the optical trap (a). In (b) the atoms were exposed to an rf sweep which populated all hyperfine states. The field of view for each image is 1.6 by 1.8 mm.

2.5.3 Propagation of Sound in a Bose-Einstein Condensate

The study of quantum liquids has revealed a wealth of physics such as superfluidity, second sound, and quantized vortices. A microscopic picture of these macroscopic quantum phenomena was developed based on elementary excitations and quantum hydrodynamics. For a long time such studies were limited to He-3 and He-4. The realization of Bose-Einstein condensation in atomic vapors has provided a new class of macroscopic quantum fluids which are dilute gases. An important issue, which applies both to quantum liquids and quantum gases, is the characterization of the system by its collective excitations.

Previous experiments on Bose condensed clouds had focused on the lowest collective excitations.[37] They show a discrete spectrum due to the small size of the trapped clouds, in contrast to the continuous spectrum of quantum liquids, which is phonon-like at low frequencies. In this study, we observed sound propagation in a Bose condensate.[38] Localized density perturbations, much smaller than the size of the condensate, were induced by suddenly modifying the trapping potential using the optical dipole force of a focused laser beam (Figure 14). The resulting propagation of sound was directly observed using a novel technique, rapid sequencing of nondestructive phase-contrast images (Figure 15). The speed of sound was determined as a function of density and found to be consistent with the predictions of Bogoliubov theory,[39] which has been formulated 50 years ago, but had not been directly tested thus far.

36 D.M. Stamper-Kurn, M.R. Andrews, A. Chikkatur, S. Inouye, H.-J. Miesner, J. Stenger, and W. Ketterle, "Optical Confinement of a Bose-Einstein Condensate," *Phys. Rev. Lett.* 80: 2027 (1998).

37 M.-O. Mewes, M.R. Andrews, N.J. van Druten, D.M. Kurn, D.S. Durfee, C.G. Townsend, and W. Ketterle, "Collective Excitations of a Bose-Einstein condensate in a Magnetic Trap," *Phys. Rev. Lett.* 77: 988 (1996); D.S. Jin, J.R. Ensher, M.R. Matthews, C.E. Wieman, and E.A. Cornell, "Collective Excitations of a Bose-Einstein Condensate in a Dilute Gas," *Phys. Rev. Lett.* 77: 420 (1996).

38 M.R. Andrews, D.M. Kurn, H.-J. Miesner, D.S. Durfee, C.G. Townsend, S. Inouye, and W. Ketterle, "Propagation of Sound in a Bose-Einstein Condensate," *Phys. Rev. Lett.* 79: 553 (1997).

39 N.N. Bogoliubov, "On The Theory of Superfluidity," *J. Phys. (USSR)* 11: 23 (1947).

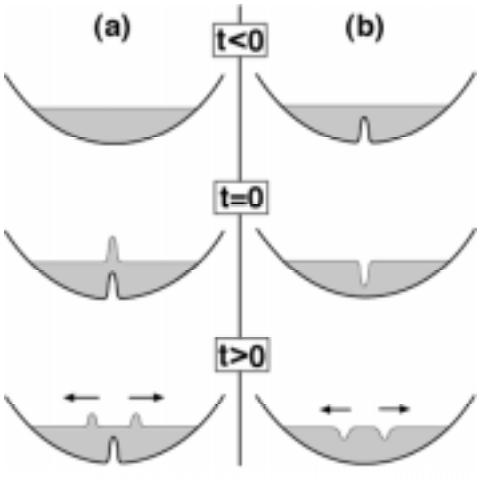

Figure 14. Excitations of wave packets in a Bose condensate. A condensate is confined in the potential of a magnetic trap. At time t=0, a focused, blue-detuned laser beam is suddenly switched on (a) or off (b) and, by the optical dipole force, creates respectively two positive or negative perturbations in density which propagate at the speed of sound.

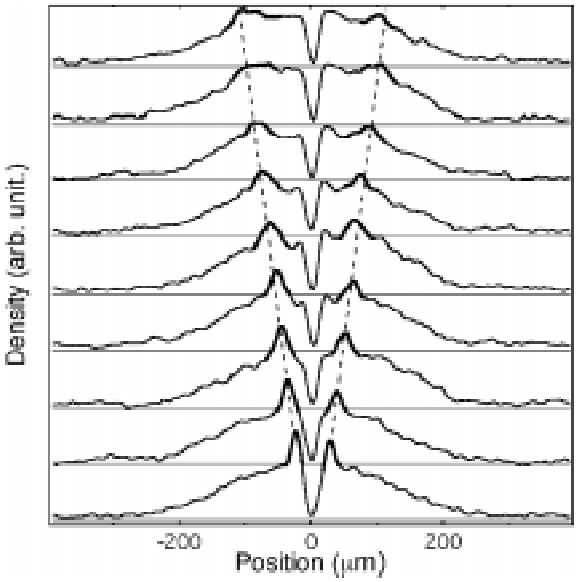

Figure 15. Observation of sound propagation in a condensate by non-destructive rapid phase-contrast imaging. Shown are axial density profiles of the condensate, taken every 1.3 ms, beginning 1 ms after switching on the argon ion laser. Two pulses traveled outward with the speed of sound (compare with Figure 14).

2.5.4 Collective Excitations at Non-zero Temperature: a Study of Zeroth, First, and Second Sound

Collective excitations are the fingerprints of a system and reveal many of its dynamic properties. We have extended earlier work on collective excitations of a Bose-Einstein condensate by studying them at non-zero temperature and at high density where they become analogous to first and second sound.[40] The existence of such two modes is characteristic for a superfluid system.

Our study focused on the lowest-lying shape oscillation (Figure 16). This oscillation was probed above and below the Bose-Einstein condensation temperature. The temperature dependencies of the frequency and damping rates (Figure 17) of condensate oscillations indicate significant interactions between the condensate and the thermal cloud. Hydrodynamic oscillations of the thermal cloud were observed, constituting first sound. An antisymmetric dipolar oscillation of the thermal cloud and the condensate was studied. This excitation represents the bulk flow of a superfluid through the normal fluid and has similarities to second sound. The detailed description of these results is currently a challenge for many-body theory.

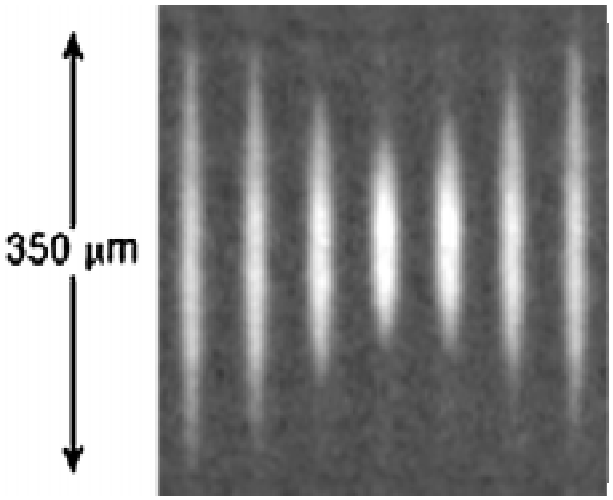

Figure 16. *In situ* images of the m = 0 quadrupolar condensate oscillation near 30 Hz. A Bose-Einstein condensate with no discernible thermal component was imaged every 5 ms by phase-contrast imaging. The evident change in the axial length of the condensate was used to characterize the oscillation.

40 D. Stamper-Kurn, H.-J. Miesner, S. Inouye, M.R. Andrews, and W. Ketterle, "Excitations of a Bose-Einstein Condensate at Non-Zero Temperature: A Study of Zeroth, First, and Second Sound," submitted to *Phys. Rev. Lett.*

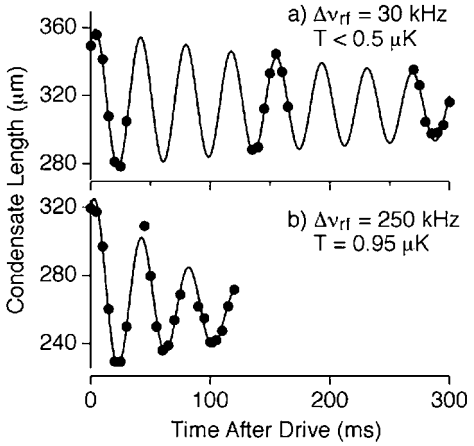

Figure 17. Damped quadrupolar condensate oscillations at low (a) and high (b) temperature. Points show the axial condensate length determined from fits to phase-contrast images (such as shown in Figure 16). The oscillation at high temperature has a slightly lower frequency and is damped more rapidly than at low temperature.

2.5.5 Bosonic Stimulation in the Formation of a Bose-Einstein Condensate

Quantum-mechanical symmetry leads to bosonic stimulation, i.e., the probability that other atoms scatter into the condensate is proportional to the number of condensed atoms already present. This process is analogous to stimulated emission of photons and constitutes "matter wave amplification." When we observed the formation of the condensate after suddenly quenching the cloud below the transition temperature (Figure 18), evidence for bosonic amplification was obtained.[41] Bosonic stimulation leads to an acceleration of the rate at which atoms enter the condensate—the formation process therefore starts slowly, speeds up and then approaches equilibrium, as was observed in Figure 18.

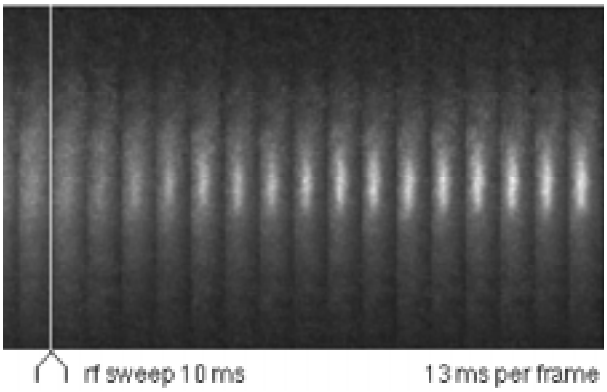

Figure 18. The formation of a Bose-Einstein condensate. Shown is a sequence of 18 phase-contrast images taken *in situ* of the same condensate. The first two frames show a thermal cloud at a temperature above the transition temperature. The following 16 frames were taken after the cloud was quenched below the BEC transition and show the growth of a condensate at the center of the cloud at 13 ms intervals. Note the decrease in the number of thermal atoms and their smaller width after the rf sweep. The bright gray levels mark the high column density of the condensate. The length of the images is 630 μm.

2.5.6 Second-order Coherence of a Bose-Einstein Condensate

The interference observed between two Bose-Einstein condensates[42] demonstrated clearly the long-range coherence of a Bose condensate.[43] The fringe contrast is directly related to first-order coherence. Our paper[44] showed that previous measurements of the interaction energy of a condensate can be reinterpreted as a measure for second-order coherence and therefore provide direct evidence for the suppression of density fluctuations in a condensate compared to a thermal cloud. The same conclusion was reached for third-order coherence, which was measured through the observation of three-body collisions.[45]

41 H.-J. Miesner, D.M. Stamper-Kurn, M.R. Andrews, D.S. Durfee, S. Inouye, and W. Ketterle, "Bosonic Stimulation in the Formation of a Bose-Einstein Condensate," *Sci.* 279: 1005 (1998).

42 W. Ketterle et al., *RLE Progress Report* 139: 222 (1996).

43 M.R. Andrews, C.G. Townsend, H.-J. Miesner, D.S. Durfee, D.M. Kurn, and W. Ketterle, "Observation of Interference Between Two Bose Condensates," *Sci.* 275: 637 (1997).

44 W. Ketterle and H.-J. Miesner, "Coherence Properties of Bose-Einstein Condensates and Atom Lasers," *Phys. Rev. A* 56: 3291 (1997).

45 E.A. Burt, R.W. Ghrist, C.J. Myatt, M.J. Holland, E.A. Cornell, and C.E. Wieman, "Coherence, Correlations, and Collisions: What One Learns About Bose-Einstein Condensates from Their Decay," *Phys. Rev. Lett.* 79: 337 (1997).

2.5.7 A Next-generation BEC Experiment

A major effort of our group is the design and construction of an improved source of Bose condensed atoms. The design includes a recirculating sodium beam oven and an improved Zeeman slower which should result in one to two orders of magnitude improvements in the loading rates of atoms traps and lead to considerably larger condensates than have been obtained so far. The trapping chamber will be a glass cell with high quality windows which will allow high resolution imaging at short working distances. Major parts of the experiment have already been assembled and are currently being tested.

2.5.8 Two-step Condensation of the Ideal Bose Gas in Highly Anisotropic Traps

The ideal Bose gas in a highly anisotropic harmonic potential was studied.[46] It was found that Bose-Einstein condensation occurs in two distinct steps as the temperature is lowered. In the first step the specific heat shows a sharp feature, but the system still occupies many one-dimensional quantum states. In the second step, at significantly lower temperature, the ground state becomes macroscopically occupied. It should be possible to verify these predictions using present-day atom traps. The two-step behavior can occur in a rather general class of anisotropic traps, including the box potential.

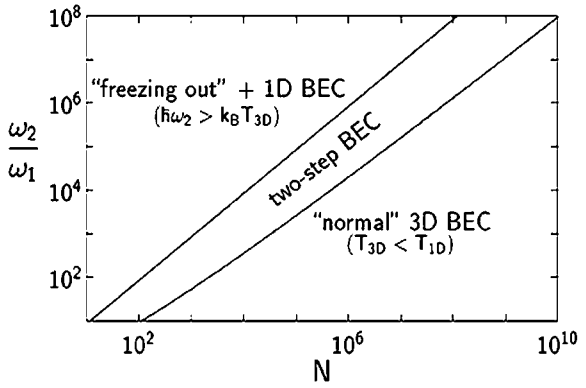

Figure 19. Overview of the three different regimes of BEC in an anisotropic harmonic oscillator potential with $\omega_1 << \omega_2 = \omega_3$ as a function of particle number N and trap anisotropy ω_2/ω_1. The two-step BEC regime separates the regime of "normal" three-dimensional BEC and the regime of extreme anisotropy where the system first becomes one-dimensional and then undergoes 1D BEC.

2.5.9 Publications

Journal Articles

Andrews, M.R., D.S. Durfee, S. Inouye, D.M. Kurn, H.-J. Miesner, and W. Ketterle. "Studies of Bose-Einstein Condensates." *Proceedings of the Symposium on Quantum Fluids and Solids* (QFS 97), Paris, July 20-26, 1997; *J. Low Temp. Phys.* 110: 153-66 (1998).

Andrews, M.R., D.M. Kurn, H.-J. Miesner, D.S. Durfee, C.G. Townsend, S. Inouye, and W. Ketterle. "Propagation of Sound in a Bose-Einstein Condensate." *Phys. Rev. Lett.* 79: 549-52 (1997).

Durfee, D.S., and W. Ketterle. "Experimental Studies of Bose-Einstein Condensation." *Opt. Express* 2: 299 (1998).

Ketterle, W., and H.-J. Miesner. "Coherence properties of Bose-Einstein Condensates and Atom Lasers. *Phys. Rev. A* 56: 3291-93 (1997).

Mewes, M.-O., M.R. Andrews, D.M. Kurn, D.S. Durfee, C.G. Townsend, and W. Ketterle. "Output Coupler for Bose-Einstein Condensed Atoms." *Phys. Rev. Lett.* 78: 582-85 (1997).

Miesner, H.-J., and W. Ketterle. "Bose-Einstein Condensation In Dilute Atomic Gases." *Proceedings of the Symposium on the Advancing Frontiers of Condensed Matter Science,* Philadelphia, October 13-14, 1997; submitted to *Solid State Comm.*

Miesner, H-J., D.M. Stamper-Kurn, M.R. Andrews, D.S. Durfee, S. Inouye, and W. Ketterle. "Bosonic Stimulation in the Formation of a Bose-Einstein Condensate." *Sci.* 279: 1005-07 (1998).

Stamper-Kurn, D., H.-J. Miesner, S. Inouye, M.R. Andrews, and W. Ketterle. "Excitations of a Bose-Einstein Condensate at Non-Zero Temperature: A Study of Zeroth, First, and Second Sound." Submitted to *Phys. Rev. Lett.*

Stamper-Kurn, D.M., M.R. Andrews, A. Chikkatur, S. Inouye, H.-J. Miesner, J. Stenger, and W. Ketterle. "Optical Confinement of a Bose-Einstein Condensate." *Phys. Rev. Lett*. 80: 2027 (1998).

van Druten, N.J., and W. Ketterle. "Two-Step Condensation of the Ideal Bose Gas in Highly Anisotropic Traps." *Phys. Rev. Lett.* 79: 553-56 (1997).

Conference Papers

Andrews, M.R., D.S. Durfee, S. Inouye, D.M. Kurn, H.-J. Miesner, and W. Ketterle. "Studies of Bose-

46 N.J. van Druten and W. Ketterle, "Two-Step Condensation of the Ideal Bose Gas In Highly Anisotropic Traps," *Phys. Rev. Lett.* 79: 553 (1997).

Einstein Condensates." *Proceedings of the International Conference on Macroscopic Quantum Coherence,* Boston, July 11-13, 1997. Forthcoming.

Miesner, H.-J., and W. Ketterle. "Bose-Einstein Condensation in Dilute Atomic Gases and Realization of an Atom Laser." *SPIE Conference Photonics West,* San Jose, California, January 24-30, 1998. Forthcoming.

Townsend, C.G., N.J. van Druten, M.R. Andrews, D.S. Durfee, D.M. Kurn, M.-O. Mewes, and W. Ketterle. "Bose-Einstein Condensation of a Weakly Intracting Gas." In *Atomic Physics 15*, Fifteenth International Conference on Atomic Physics, Amsterdam, August 1996. *Singapore: World Scientific*, 1997, pp. 192-211.

Popular Articles

Ketterle, W. "Atom Laser." In *McGraw-Hill's 1999 Yearbook of Science and Technology,* companion volume to *Encyclopedia of Science and Technology.* New York: McGraw-Hill. Forthcoming.

Ketterle, W. "Bose-Einstein-Kondensate—Eine neue Form von Quantenmaterie." *Phys. B.* 53: 677-80 (1997).

Townsend, C.G., W. Ketterle, and S. Stringari. *"Kondensacja Bosego-Einsteina."* (Polish translation of the *Physics World* article). *Postepy Fizyki* 48: 333-50 (1997).

Townsend, C.G., W. Ketterle, and S. Stringari. "La Condensazione di Bose-Einstein." (Italian translation of the *Physics World* article). *Le Scienze* 347: 60-65 (1997).

Townsend, C.G., W. Ketterle, and S. Stringari. "Bose-Einstein Condensation." *Physics World,* March: 29-34 (1997).

Published Abstracts from Conference Papers Presented

Andrews, M.R., C.G. Townsend, H.-J. Miesner, D.S. Durfee, D.M. Kurn, and W. Ketterle. "Observation of Interference Between Bose-Einstein Condensates." *Bull. Am. Phys. Soc.* 42: 1095 (1997).

Ketterle, W. "I.I. Rabi Prize Lecture: Bose-Einstein Condensates—Matter with Laser-like Properties." *Bull. Am. Phys. Soc.* 42: 941 (1997).

Ketterle, W. "Recent Experimental Results with Bose Condensed Atoms." Symposium on Quantum Fluids and Solids (QFS 97), Paris, July 20-26, 1997; Book of Abstracts, D-I1.

Ketterle, W. "Latest Results in Bose-Einstein Condensation." Quantum Electronics and Laser Science Conference (QELS), Baltimore, Maryland; *OSA Tech. Digest Series* 12: 24 (1997).

Ketterle, W. "Bose-Einstein Condensates—'Laser-like' Atoms." Institute of Physics Congress, Program and Abstracts, 1997, p. 5.

Ketterle, W. "Bose-Einstein-Kondensate—Eine neue Form von Quantenmaterie." *Verhandl. DPG* (VI) 32: 410 (1997).

Ketterle, W. "Bose-Einstein Condensation in Trapped Atomic Na." *Bull. Am. Phys. Soc.* 42: 798 (1997).

Ketterle, W. "When Atoms Behave as Waves: Bose-Einstein Condensation and the Atom Laser." 1997 OSA Annual Meeting, *Book of Abstracts,* WY1.

Kurn, D.M., M.R. Andrews, H.-J. Miesner, D.S. Durfee, C.G. Townsend, S. Inouye, and W. Ketterle. "Studies of Coherence of Bose-Einstein Condensation." OSA Annual Meeting, 1997, Book of Abstracts, WFF16.

Kurn, D.M., H.-J. Miesner, M.R. Andrews, D.S. Durfee, C.G. Townsend, S. Inouye, C. Kuklewicz, and W. Ketterle. "Collective Excitations and the Nature of Sound in a Bose Condensed Gas." OSA Annual Meeting, 1997, *Book of Abstracts,* WNN3.

Kurn, D.M., M.R. Andrews, D.S. Durfee, C.G. Townsend, H.-J. Miesner, M.-O. Mewes, and W. Ketterle. "Techniques for Probing and Manipulating Bose-Einstein Condensates." Quantum Electronics and Laser Science Conference (QELS), Baltimore, Maryland, 1997; *OSA Tech. Digest Series* 12: 105 (1997).

Mewes, M.-O., M.R. Andrews, C.G. Townsend, H.-J. Miesner, D.S. Durfee, D.M. Kurn, and W. Ketterle. "Bose-Einstein-Kondensate—Eine neue Form der Quantenmaterie." *Verhandl. DPG (VI)* 32: 348 (1997).

Thesis

Mewes, M.-O. *Bose-Einstein Condensation of Sodium Atoms.* Ph.D. diss., Department of Physics, MIT, 1997.